ELSEVIER

Chemical Engineering and Processing 36 (1997) 489–495

Chemical Engineering and Processing

Experimental study of a cocurrent upflow packed bed bubble column reactor: pressure drop, holdup and interfacial area

E.J. Molga [1], K.R. Westerterp *

Department of Chemical Engineering, Chemical Reaction Engineering Laboratories, Twente University, P.O. Box 2177, 7500 AE Enschede, Netherlands

Received 3 March 1997; received in revised form 4 June 1997; accepted 9 June 1997

Abstract

Gas–liquid interfacial areas have been determined by means of chemically enhanced absorption of CO_2 into DEA in a packed bed bubble column reactor with an inner diameter of 156 mm. The influence of the gas velocity and particle diameter on the interfacial areas, pressure drops and liquid holdups has been investigated. For both packings the limiting values of the gas velocities have been determined above which the interfacial areas and liquid holdups stabilize. In particular gas channelling has been found, which is less pronounced in the bed of larger particles. © 1997 Elsevier Science S.A.

Keywords: Bed bubble column; Interfacial area; Pressure drop

1. Introduction

The study described is a continuation of our previous investigations of the interfacial area, liquid holdup and pressure drop in a packed bed bubble column reactor at elevated pressures, see Molga and Westerterp [1]. In the cited paper the influence of pressure and gas and liquid velocities on the specific gas–liquid interfacial area as well as on the liquid holdup and the pressure drop is reported as measured in a column of a diameter of $D = 156$ mm and for three sizes of the spherical packing particle diameter of $d_p = 2$, 4.2 and 10 mm, respectively. An analysis of the results obtained led to the following conclusions:

- the influence of the reactor pressure is more noticeable for the holdup than for the interfacial areas. The liquid holdup β_L decreases when the reactor pressure increases,
- interfacial areas increase and liquid holdups decrease for increasing gas velocities,
- models based on flow patterns indicate that gas channeling is significant in our system,
- the flow maldistribution becomes more significant for smaller packing particle diameters.

The superficial gas velocities used in the above cited study ranged between $10 < u_{Go} < 70$ mm s^{-1}. The small gas velocities were limited by the capacity of the booster used to circulate the gas: at an operating pressure of 6.4 MPa: a gas mass flow rate as large as 4.8 kg min^{-1} was needed for a superficial gas velocity of 60 mm s^{-1} in the column.

We decided to check the gas channelling and the influence of the packing particle diameter on flow maldistributions as well as on the interfacial areas at higher gas velocities. In the present study experimental runs have been made at superficial gas velocities up to 200 mm s^{-1} and at operating pressures of $0.05 < P < 0.2$ MPa for particle diameters of 4.2 and 10 mm, respectively. Results will be compared to those determined previously at elevated pressures.

2. Experimental

Chemically enhanced absorption of CO_2 in nitrogen as a carrier gas into aqueous solutions of diethanolamine (DEA) has been used for the determination of interfacial areas as described earlier, see Molga and Westerterp [1]. Also the same experimental installa-

* Corresponding author. Tel.: +31 53 4892877; fax: +31 53 4894738.

[1] Permanent address: Warsaw Technical University Chemical and Process Engineering ul. Warynskiego 1, 00-645 Warszawa, Poland

PII S0255-2701(97)00026-3

tion and procedures, described in detail in the cited paper, have been used. In this study to increase the gas velocity in the column an additional gas booster, a gas driven Resato compressor, type DBS-115-1, has been installed. The main operating conditions and bed parameters are listed in Table 1.

3. Results

3.1. Flow regime

The location of our experimental points in the flow map of Turpin and Huntington [2] as well as that of Fukushima and Kusaka [3] indicates that according to the criteria of Turpin and Huntington our measurements have been made in the transition region between the bubble, slug and spray regimes while following the criteria of Fukushima and Kusaka our experimental points for both series are in a churn flow regime. Visual observations during experimental runs indicated we operated in the bubble flow regime with, at the highest gas velocities, an increasing contribution of churn and pulsations. The pulsations were particularly noticeable in the column filled with particles of $d_p = 10$ mm. The structure of the gas–liquid flow in the packed beds will be discussed in more detail below.

3.2. Pressure drop in the column

The frictional pressure drop per unit length of the bed $(\Delta P/L)_{\text{frictional}}$ have been calculated from the total pressure drop $(\Delta P/L)_{\text{total}}$ as measured with a differential pressure cell. A correction for the hydrostatic pressure of the gas–liquid mixture present in the bed has been applied according to the following relationship:

$$\left(\frac{\Delta P}{L}\right)_{\text{frictional}} = \left(\frac{\Delta P}{L}\right)_{\text{total}} - \rho_L \beta_L g - \rho_G (1-\beta_L) g \qquad (1)$$

Eq. (1) is valid for uniform flow patterns in the bed, i.e. in absence of radial pressure gradients. Because of the gas channelling detected in our packed beds we expect local radial pressure gradients to be present; this has not been taken into account in Eq. (1), so the values of $(\Delta P/L)_{\text{frictional}}$ calculated with Eq. (1) have to be considered as overall values.

Table 1
Main operating conditions and bed properties

Column pressure	$P = 0.05/0.22$	[MPa]
Superficial gas velocity	$u_{Go} = 14/188$	[mm s^{-1}]
Superficial liquid velocity	$u_{Lo} = 0.1/0.45$	[mm s^{-1}]
Concentration of DEA in water	$C_{DEA} = 1.5$	[mol kg^{-1}]
Particle (glass spheres) diameter	$d_p = 4.2$ and 10	[mm]
Bed length	$L = 0.47$	[m]

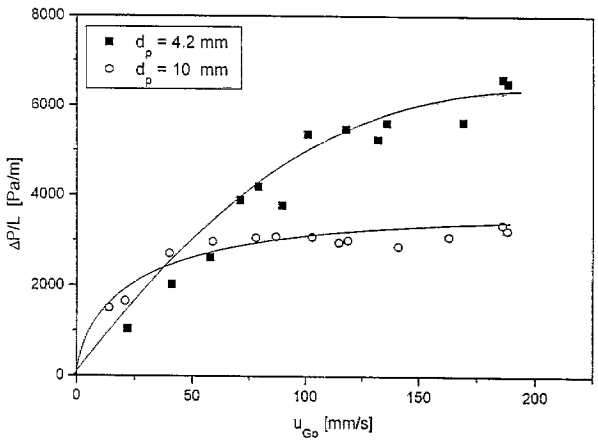

Fig. 1. Frictional pressure drop as a function of the gas superficial velocity.

The resulting frictional pressure gradients calculated with Eq. (1) are plotted in Fig. 1 as a function of the superficial gas velocity. For the particle diameter of $d_p = 10$ mm and above gas velocities of 60 mm s^{-1} the pressure gradient becomes weakly dependent on the gas velocity. A similar but less pronounced trend can be also observed for the packing with $d_p = 4.2$ mm, where the pressure gradient becomes weakly dependent on gas velocities above of around 100 mm s^{-1}.

The frictional pressure drop in two-phase flow through packed beds consists of three contributions: gas–liquid interfacial dissipation, liquid-packing frictional dissipation and gaspacking frictional dissipation in the not wetted channels. Usually, at conditions typical for upflow packed bubble columns the first two components dominate and the contribution of the gaspacking frictional dissipation is negligible. The behaviour observed in Fig. 1 may indicate that at the limiting gas velocities the flow patterns in the bed stabilize, which means that further increase of the gas velocity above these limiting values does not influence the two-phase flow hydrodynamics in the bed anymore. Because of the contribution of frictional gas–solid dissipation being negligible the observed overall frictional pressure drops stabilize in this region. Two-phase flow patterns in the packed bed will be discussed below in more detail. The pressure drop in two-phase flow through packed columns is usually expressed as a gas–liquid friction factor f_{LG} defined as follows:

$$f_{LG} = \frac{(\Delta P/L) d_{pe}}{2\rho_G u_{Go}^2} \qquad (2)$$

where d_{pe} is the equivalent particle diameter. d_{pe} may be defined as a hydraulic diameter:

$$d_{pe} = d_H = \frac{2}{3}\frac{d_p \varepsilon}{1-\varepsilon} \qquad (3)$$

Also other definitions of d_{pe} are in use e.g. the one given by Krischer and Kast [4]:

$$d_{pe} = d_H* = d_p\left(\frac{16\varepsilon^3}{9\pi(1-\varepsilon)^2}\right)^{1/3} \quad (4)$$

The friction factor f_{LG}, based on d_H as in Eq. (4), is shown in Fig. 2 as a function of the gas velocity. The points for both particle diameters lay along the same correlation line. As can be observed in the diagram at gas velocities higher than 100 mm s^{-1} the friction factor for our system decreases very slowly. Turpin and Huntington [2] correlated the friction factor f_{LG}, calculated with d_H of Eq. (3), as the following function of a parameter Z:

$$\ln f_{LG} = 8 - 1.12 \ln Z - 0.0769(\ln Z)^2 + 0.0152(\ln Z)^3 \quad (5)$$

for $0.3 < Z < 500$ the parameter Z is defined as:

$$Z = \frac{Re_G^{1.167}}{Re_L^{0.767}} \quad (6)$$

Values of f_{LG} obtained from measurements plotted in Z coordinates to compare them with the correlation of Turpin and Huntington indicate the parameter Z as defined in Eq. (6) is not a proper measure to correlate our experimental pressure drop data. Larachi et al. [5] propose to correlate the pressure drop in the form of the equation:

$$f_{LG} = \frac{1}{\lambda^{1.5}}\left(45.6 + \frac{15.9}{\lambda^{0.5}}\right) \quad (7)$$

where the parameter λ is defined as follows:

$$\lambda = \chi(Re_L We_L)^{0.25} \quad (8)$$

and the inertial Lockhart–Martinelli factor χ reads as:

$$\chi = \frac{u_{Go}}{u_{Lo}}\left(\frac{\rho_G}{\rho_L}\right)^{0.5} \quad (9)$$

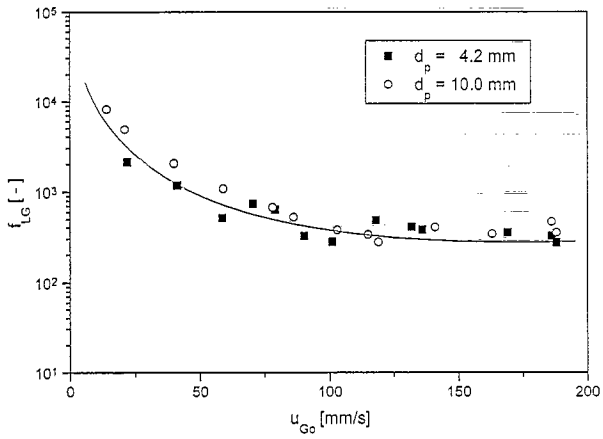

Fig. 2. Friction factor f_{LG} as a function of the gas superficial velocity.

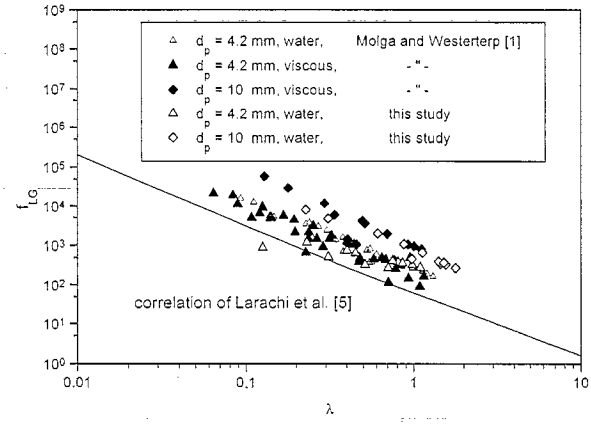

Fig. 3. Friction factor f_{LG} as a function of the parameter λ (Eq. (8)).

The Reynolds number and the Weber number for liquids are equal to $Re_L = u_{Lo}d_p\rho_L/\mu_L$ and $We_L = u_{Lo}^2 d_p\rho_L/\sigma_L$, respectively. The dependence of the friction factor f_{LG} on the parameter is shown in Fig. 3. Also results obtained in our previous study, see Molga and Westerterp [1], as well as the correlation of Larachi et al. [5], see Eq. (7), are shown in the diagram. No influence of the liquid viscosity is noticed but there is a distinct influence of d_p indeed. For both our studies the experimental data are situated above the correlation line of Larachi et al. [5]: for a given λ value our f_{LG} values are up to 50 times higher. These discrepancies may be caused by scaling-up effects, because most experimental points collected by Larachi et al. [5] concern particles and column diameters smaller than those used in our study, although some of their data also refer to columns with 23 and 235 mm diameter respectively. Our particle diameters were 4 and 10 mm and those of Larachi et al. [5,6] are mostly smaller than 3 mm. The Larachi correlation does not hold for larger particles.

3.3. Liquid holdups

Values of liquid holdups in the bed of $d_p = 10$ mm are plotted in Fig. 4. Data at elevated pressures, measured previously [1], are also plotted in the diagram. We can observe that p_L tends to stabilize at higher gas velocities. Following the concept proposed by Larachi et al. [7] our holdup data have also been correlated as the drift flux J_{DF} defined as:

$$J_{DF} = u_{Go}\beta_L - u_{Lo}(1-\beta_L) \quad (10)$$

which is a unique function of the gas velocity. The drift fluxes as calculated with the experimental data of p_L have been plotted in Fig. 5. For comparison our data obtained previously at lower gas velocities and at elevated pressures [1] are also given. At velocities higher than 100 and 40 mm s^{-1} for $d_p = 10$ and 4.2 mm,

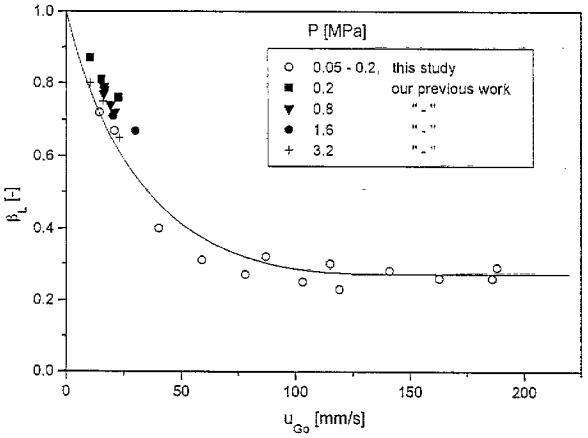

Fig. 4. Liquid holdups in the bed of $d_p = 10$ mm. Comparison to the data obtained at elevated pressures-see Molga and Westerterp [1].

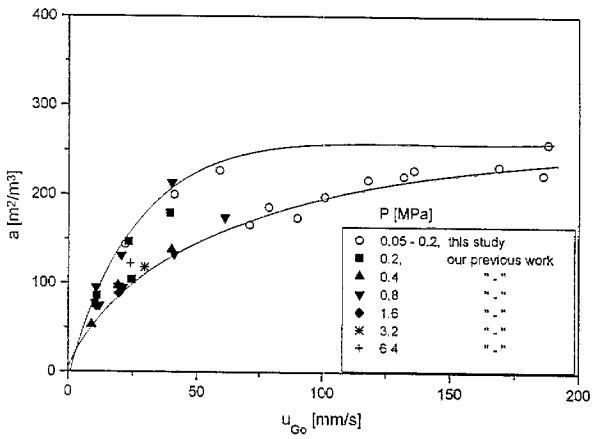

Fig. 6. Interfacial areas obtained in the bed of $d_p = 4.2$ mm. Comparison to the data obtained at elevated pressures.

respectively, a systematic deviation from the correlation line is noticed.

3.4. Interfacial areas

Determined interfacial areas are plotted in Figs. 6–9. In Figs. 6 and 7 also our data obtained previously at elevated pressures and at lower gas velocities are included. We can observe in the diagram values of determined interfacial areas at the highest gas velocities stabilize and are very close to each other for both diameters of d_p. Subsequently, interfacial areas related to the specific surface area of the packing as a/a_s are shown in Fig. 8. We observe the relative interfacial areas are much higher for the larger packing particles. Midoux et al. [7] proposed the following correlations for interfacial areas:

$$a = 374\varepsilon\left(\frac{\varepsilon^2}{a_s}\frac{\zeta_{LG}}{u_{Lo}+u_{Go}}\right)^{0.65} \tag{11}$$

where ζ_{LG} iS the power dissipated per unit volume of the voids defined as follows:

$$\zeta_{LG} = \frac{1}{\varepsilon}(u_{Lo}+u_{Go})\frac{\Delta P}{L} + \frac{u_{Lo}\rho_L + u_{Go}\rho_G}{\varepsilon}g \tag{12}$$

This correlation derived previously for cocurrent downflow in packed columns, was also successfully applied to upflow systems, see Lara Marquez et al. [8]. A comparison of our experimental interfacial areas to those predicted with the correlation Eq. (11) is shown in Fig. 9. We observe most of the experimental points lay within the confidence limits, although points for different d_p are grouped separately.

Lara Marquez et al. [8] have also proposed a correlation based on the relation between the Kolmogoroffmicroscale of turbulence and the power dissipation rate ζ_{LG}. For our system this correlation predicts interfacial areas much less accurately than that of Midoux et al. [7].

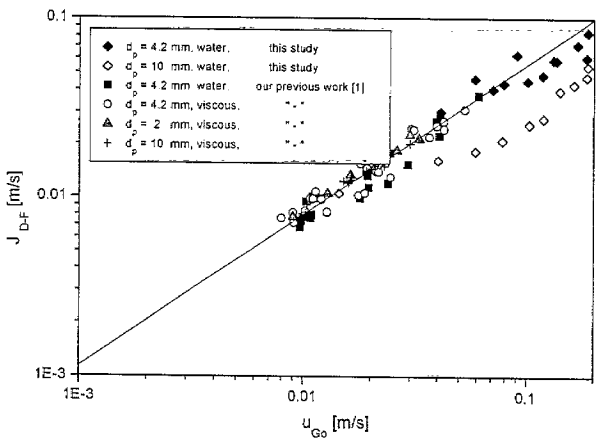

Fig. 5. Drift flux J_{DF} as a function of the gas superficial velocity.

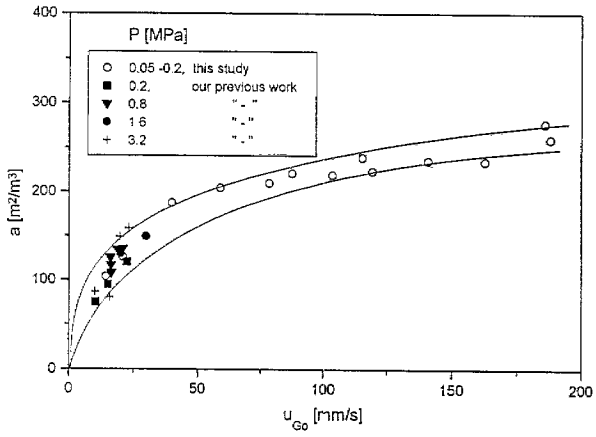

Fig. 7. Interfacial areas obtained in the bed of $d_p = 10$ mm. Comparison to the data obtained at elevated pressures.

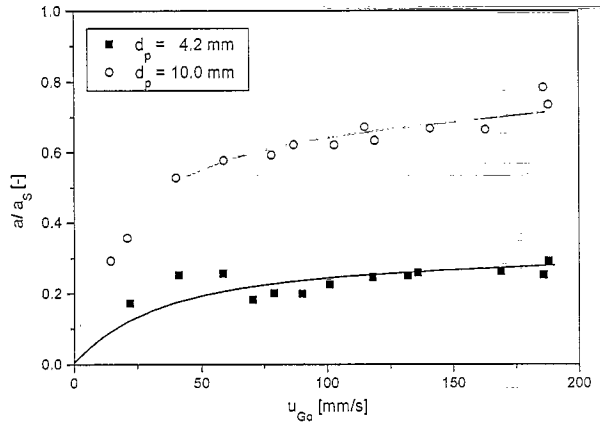

Fig. 8. Relative interfacial areas a/a_s as a function of the gas superficial velocity.

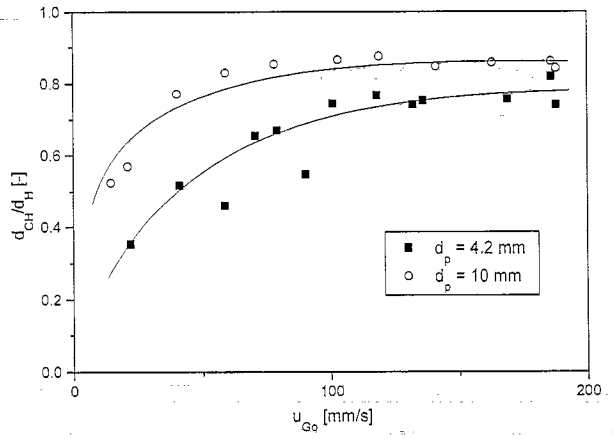

Fig. 10. Ratio d_{CH}/d_H as a function of the gas superficial velocity.

4. Discussion

In accordance to the analysis presented previously [1] two limiting flow patterns can be considered for uniform (without maldistributions) two-phase upflow: bubble flow and continuous gas streams flowing through wetted bed voids.

For bubble flow the mean Sauter bubble diameter d_S can be calculated with the experimental values of β_L and a:

$$d_S \frac{6\varepsilon(1-\beta_L)}{a} \tag{13}$$

In this study values of d_S obtained from experimental measurements are always larger than the hypothetical interparticle capillary diameter dH calculated with Eq. (3), so in the applied range of operating conditions no a 'pure' bubble flow can be expected in our column.

For the second limiting flow pattern the diameter of the gas streams flowing through wetted bed voids can be calculated as:

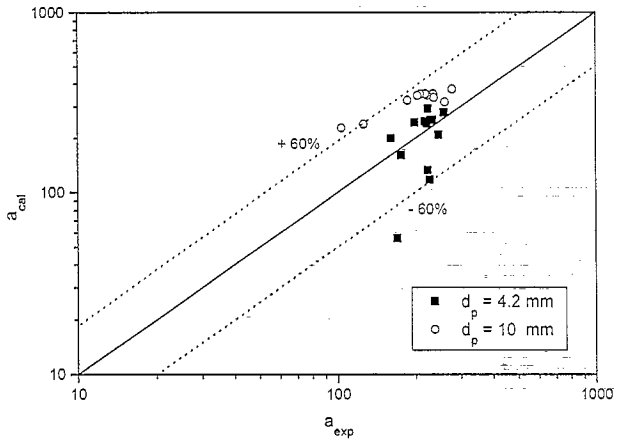

Fig. 9. Comparison of our interfacial areas to those predicted with the correlation of Midoux et al. [7].

$$d_{CH} = d_H \sqrt{(1-\beta_L)} \tag{14}$$

Values of the ratio d_{CH}/d_H calculated with experimentally determined holdups β_L are always smaller than unity as shown in Fig. 10. But the values of interfacial areas estimated for this case following the relationship:

$$a = 4\sqrt{(1-\beta_L)}\,\frac{\varepsilon}{d_H} \tag{15}$$

are always higher than the experimental ones. So also "pure" streams of only gas flow through wetted bed voids also do not occur in our column.

The above analysis indicates strong flow maldistributions are present in our system. So in parallel to the bubble flow in main part of the column either part of the channels in the bed voids (solid particle surface) is not wetted with liquid, or no gas flows through some of the interparticle channels. A contribution of each flow pattern to the total structure of two-phase flow through the packed bed is difficult to estimate without residence time distribution measurements.

The dynamic gas disengagement (DOD) method, proposed by Sriram and Mann [9] and widely employed to investigate the hydrodynamics of bubble columns, e.g. see Deckwer [10], has been applied also in this study to estimate the contribution of gas channelling to the total gas flow through the column. In the DGD method the gas and liquid feeds are stopped simultaneously and the liquid level registered as a function of time. In this way the homogeneous and heterogeneous flow fractions can be distinguished from the dynamic liquid level response. The application of this method to a packed bed bubble column is expected to be limited because of strong mutual gas–liquid–solid interactions. Representative results for the two packing particle diameters are shown in Fig. 11 where the measured liquid level H, after stopping the gas and liquid supply, is plotted. We observe strong gas–liquid–solid interactions during the dynamic measurements. These interactions are more pronounced in the bed with a particle

diameter of $d_p = 4.2$ mm where first the liquid level drops rapidly due to the gas escape and after that rises slowly due to the trickling of liquid. This effect is less pronounced for $d_p = 10$ mm. Because of the observed interactions only qualitative conclusions on the possible heterogeneous–homogeneous flow structure can be drawn—the flow structure seems be more uniform for $d_p = 10$ mm.

Also a simple analysis based on an overall volumetric balance is proposed here to characterize the flow structure in the bed. Assuming the gas–liquid interfacial contact area is surrounded by a hypothetical liquid layer of a thickness δ_L, the total volume of the liquid in the column is equal to $V_L = \delta_L a V_R$. This liquid volume V_L is also equal to $\beta_L \varepsilon V_R$, so that:

$$\delta_L = \frac{\varepsilon \beta_L}{a} \qquad (16)$$

The averaged liquid film thickness δ_L depends on the mutual gas–liquid–solid interactions in the packed bed so it may be used to characterize the flow hydrodynamics at the operating conditions. The values of δ_L obtained with Eq. (16) are plotted in Fig. 12 as a function of the power dissipation rate in the two-phase flow ζ_{LG}. At a very small energy input the values of δ_L are very close to the hydraulic diameter d_H, then with increase of ζ_{LG} they decrease and eventually stabilize. Limiting values of δ_L obtained at larger energy inputs (gas velocities) are dependent on the particle diameters—the stabilized value of δ_L is larger for $d_p = 4.2$ mm. A higher energy input is also needed for smaller packing particles to keep the flow conditions in the bed stable.

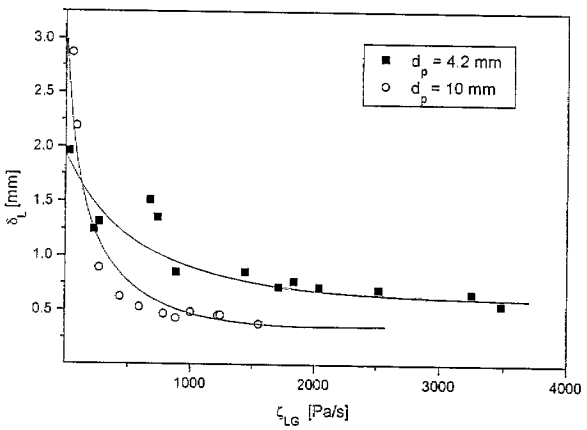

Fig. 12. Thickness of a hypothetical liquid layer δ_L as a function of ω_{LG}.

5. Conclusions

In our experimental system at the applied operating conditions the mutual gas–liquid interactions have a significant influence on the pressure drops, holdups as well as interfacial areas. While the liquid flow rate is kept constant, these interactions for a given experimental system are influenced mainly by the gas velocity. Increasing the gas velocity, liquid holdups decrease. At certain limiting values of the gas velocity p_L and a tend to stabilize. A further increase of the gas flow rate does not change the interfacial areas and liquid holdups anymore. The absolute values of the interfacial areas in the stable regime practically do not depend on the particle diameter, but the relative values alas are higher for larger particles. Significant maldistributions of the two-phase flow are detected for both investigated particle diameters they are less pronounced for $d_p = 10$ mm.

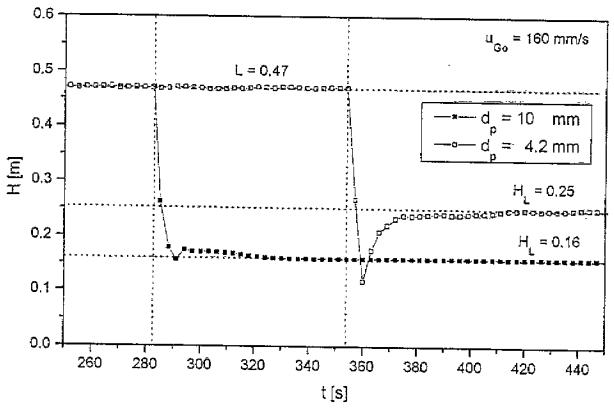

Fig. 11. Results of dynamic gas disengagement measurements for both packing particle diameters.

6. Nomenclature

a	interfacial area per unit volume of the reactor, $m^2\ m^{-3}$
a_s	specific surface area of the packing per unit volume of the reactor, $m^2\ m^{-3}$
d_{CH}	diameter of the continuous gas stream, Eq. (14), m
d_H	hydraulic diameter of a hypothetical capillary in the bed, m
d_H^*	hydraulic diameter of a hypothetical capillary in the bed, m
d_p	particle diameter, m
d_S	mean Sauter diameter of gas bubbles, Eq. (13), m
f_{LG}	two-phase friction factor, Eq. (1), —
g	acceleration due to gravity, $m\ s^{-2}$
J_{DF}	drift flux, Eq. (6), $m\ s^{-1}$
L	bed height, m
P	reactor pressure, MPa
$\Delta P/L$	frictional pressure gradient in the column, $Pa\ m^{-1}$
Re_L	$= u_{Lo} d_p \rho_L / \mu_L$—liquid Reynolds number, —

u_{Go} superficial gas velocity, m s^{-1}
u_{Lo} superficial liquid velocity, m s^{-1}
V volume, m^3
We_L $u_{Lo}^2 d_p \rho_L / \sigma_L$—liquid Weber number, —
Z flow parameter, Eq. (5), —

Greek

β holdup per unit volume of the voids, —
ε bedd porosity, —
δ_L hypothetical overall thickness of liquid layer, Eq. (16), m
λ parameter defined with Eq. (8), —
ρ density, kg m^{-3}
ζ_{LG} power dissipation rate per unit volume of interparticle voids, Eq. (12), Pa s^{-1}
χ inertial Lokhart–Martinelli factor, Eq. (9), —

Subscripts, Superscripts

G gas
L liquid
R reactor

Acknowledgements

We would very much like to thank Ing. G.H. Banis as well as A.H. Pleiter, K. van Bree and F. ter Borg of the High Pressure Laboratory for their technical support, advice and help. The investigations were financially supported by the Netherlands Organization for the Advancement of Scientific Research (NWO).

References

[1] E. Molga, K.R. Westerterp, Gas–liquid interfacial area and holdup in a cocurrent upflow packed bed bubble column reactor up to elevated pressures, Ind. Eng. Chem. Res. 36 (1997) 622–631.
[2] J.L. Turpin, R.L. Huntington, Prediction of pressure drop for two-phase, twocomponent cocurrent flow i packed beds, AIChE J 13 (1967) 1196–1202.
[3] S. Fukushima, K. Kusaka, Gas–liquid mass transfer and hydrodynamic flow region in packed columns with cocurrent upward flow, J. Chem. Eng. Jap. 12 (1979) 296–301.
[4] O. Krischer, W. Kast, Trockungstechnik, 3rd ed., Springer-Verlag, Berlin, 1978, p. 128.
[5] F. Larachi, G. Wild, A. Laurent, N. Midoux, Influence of gas density on the hydrodynamics of cocurrent gas–liquid upflow fixed bed reactors, Ind. Eng. Chem. Res. 33 (1994) 519–525.
[6] F. Larachi, A. Laurent, N. Midoux, G. Wild, Experimental study of a trickle bed reactor operating at high pressure: two-phase pressure drop and liquid saturation, Chem. Eng. Sci. 46 (1991) 1233–1246.
[7] N. Midoux, B.I. Morsi, M. Purwasasmita, A. Laurent, J.C. Charpentier, Interfacial area and liquid-side mass transfer coefficient in trickle bed reactors operating with organic liquids, Chem. Eng. Sci. 39 (1984) 781–794.
[8] A. Lara Marquez, F. Larachi, G. Wild, A. Laurent, Mass transfer characteristics of fixed beds with cocurrent upflow and downflow. A special reference to the effect of pressure, Chem. Eng. Sci. 47 (1992) 3485–3492.
[9] K. Sriram, R. Mann, Dynamic gas disengagement: a new technique for assessing the behaviour of bubble columns, Chem. Eng. Sci. 32 (1977) 571–580.
[10] W.D. Deckwer, Bubble Column Reactors, Wiley, Chichester, 1992, pp. 155–210.